confirms the absence of O=Mn^{IV}(TPP).

Interestingly, oxidation of triphenylphosphine was observed during the photolysis. In the presence of $P(C_6H_5)_3$, 1.01 (3) equiv of $OP(C_6H_5)_3$ per Mn(TPP)(OSO_3H) is formed, and with $[Mn(TPP)]_2(SO_4)$, 0.95 (5) equiv is formed. Due to the fact that metal–oxo species have already been ruled out, this oxidation to $OP(C_6H_5)_3$ most likely does not involve the porphyrin. The ultimate fate of the axial sulfate ligands could not be ascertained. On the basis of charge balance considerations, we may expect $HSO_4^{\bullet}$ or SO_4 diradical to be formed depending on the system in question. The SO_4 diradical is relatively stable toward decomposition to SO_3 and O as well as to SO_2 and O_2.[26] The HSO_4 radical can abstract a hydrogen atom from hydrocarbons,[26] but no oxidative chemistry would result. Detection of these or other possible radical species by spin-trapping was unsuccessful, due to photodecomposition of the traps themselves.

(26) Benson, S. W. *Chem. Rev.* **1978**, *78*, 23.

Conclusions

The new species $[Mn(TPP)]_2(SO_4)$ and Mn(TPP)(OSO_3H) have been synthesized, and their single-crystal X-ray structures show stereochemistry similar to that of the analogous iron complexes. Both manganese compounds are cleanly photoreduced to Mn^{II}(TPP) on irradiation in the region 350–420 nm. In contrast to other manganese oxoanion complexes, no metal–oxo species are formed and no oxidation of hydrocarbons is observed.

Acknowledgment. This work was supported by the National Institutes of Health. We thank Charlotte L. Stern of the University of Illinois X-ray Crystallographic Laboratory for help in performing the structural analyses. We gratefully acknowledge receipt of an NIH Research Career Development Award (K.S.S.) and an NIH Traineeship (R.A.W.).

Supplementary Material Available: Tables of complete atomic coordinates, thermal parameters, and complete bond distances and angles for $[Mn(TPP)]_2(SO_4)$ and Mn(TPP)(OSO_3H) (14 pages). Ordering information is given on any current masthead page.

Contribution from Rhône-Poulenc, Inc., New Brunswick, New Jersey 08901, Lawrence Berkeley Laboratory, Berkeley, California 94720, and Department of Chemistry and Molecular Structure Center, Indiana University, Bloomington, Indiana 47405

Photoreduction of Cerium(IV) in $Ce_2(O^iPr)_8(^iPrOH)_2$. Characterization and Structure of $Ce_4O(O^iPr)_{13}(^iPrOH)$

Kenan Yunlu, Peter S. Gradeff, Norman Edelstein, W. Kot, G. Shalimoff, William E. Streib, Brian A. Vaartstra, and Kenneth G. Caulton*

Received October 4, 1990

Visible irradiation of $Ce_2(O^iPr)_8(^iPrOH)_2$ yields the mixed-valence compound $Ce_4O(O^iPr)_{13}(^iPrOH)$, characterized by ^1H NMR and infrared spectra, elemental analysis, and X-ray diffraction. The structure is described as $Ce_4(\mu_4\text{-}O)(\mu_3\text{-}O^iPr)_2(\mu_2\text{-}O^iPr)_4(O^iPr)_7(^iPrOH)$. The $Ce_4(\mu_4\text{-}O)$ core has a butterfly form, with a crystallographic C_2 axis that passes through the oxide ion and the center of a symmetric hydrogen bond between the coordinated alcohol and one terminal alkoxide. This photoredox reaction cannot be thermally induced and requires that hydrogen be present on the carbon α to the alkoxide oxygen. Magnetic susceptibility and EPR studies show the compound to be paramagnetic. Two temperature ranges of Curie–Weiss behavior are observed with $\mu_{eff} = 2.7\ \mu_B$ from 80 to 300 K. Crystal data (−130 °C): a 21.405 (6) Å, b = 14.077 (3) Å, c = 20.622 (6) Å, and β = 103.97 (1)° with $Z = 4$ in space group $C2/c$.

Introduction

Cerium(IV) has a long tradition as an oxidant in organic chemistry.[1-4] Under acidic aqueous conditions, ethanol is oxidized to acetaldehyde and cyclohexanol to cyclohexanone.[1] In addition to these thermal reactions, photopromotion of certain oxidations has been demonstrated,[5] and Ce(IV) has also been employed in a photolytic splitting of water to give Ce(III), O_2, and H^+.[6] It is reported that the oxidation of methanol to formic acid by Ce(IV) is greatly enhanced by light.[7]

Against this background stands the isolable compound $Ce_2(O^iPr)_8(^iPrOH)_2$,[8,9] which is "stable to about 200 °C under vacuum".[1] We have found that ^{i}PrOH solutions of this compound are photosensitive, and we report here the nature of the product of this reaction.

Experimental Section

All procedures were carried out under an atmosphere of dry dinitrogen or argon or in vacuo. All solvents were appropriately dried and distilled prior to use and stored under dinitrogen.

Infrared spectra were recorded on a Perkin-Elmer 283B spectrometer as Nujol mulls. NMR spectra (^1H, $^{13}C\{^1H\}$) were recorded on Bruker AM-500, WH-90, and AC-200 and JEOL FX 90Q spectrometers and chemical shifts referenced to the protio impurity of the solvent. Elemental analyses were performed at Dornis and Kolbe and Oneida Research Services.

Synthesis of $Ce_4O(O^iPr)_{13}(^iPrOH)$. A solution of $Ce_2(O^iPr)_8(^iPrOH)_2$[8,9] (10 g) in a 2:1 mixture of $MeOC_2H_4OMe/^iPrOH$ (50 mL) was exposed to sunlight for 50 h (not optimized). The color changed to olive green and then orange-brown. Separate experiments in toluene-d_8 showed that, within the first 5 h of photolysis, the sharp ^1H NMR doublet of $Ce_2(O^iPr)_8(^iPrOH)_2$ at 1.28 ppm has converted into a broad singlet at 1.18 ppm, and the final broad singlet spectrum (0.15 ppm) was achieved within 20-h irradiation time. Storage of the reaction solution at −30 °C for 48 h gave orange-brown crystals. Yield: 3.3 g (41%). Anal. Calcd for $C_{42}H_{99}Ce_4O_{15}$: C, 35.91; H, 7.05; Ce, 39.94. Found, C, 36.24; H, 6.81; Ce, 39.82. IR (Nujol mull, cm^{-1}): 3150 (w), 1327 (m), 1152 (sh), 1121 (vs), 982 (vs), 968 (vs), 950 (s), 828 (m), 712 (m), 520 (m), 495 (m), 439 (m). $^{13}C\{^1H\}$ NMR (25 °C, toluene-d_8): 26.85, 71.76. ^1H NMR (500 MHz, toluene-d_8): At 305 K, the dominant species gave a broad resonance centered at δ 0.20, spanning approximately 5 ppm. A sharper resonance at δ 6.00 was also observed, as well as resonances attributed to $Ce_2(O^iPr)_8(HO^iPr)_2$, present as an impurity. As the solution was cooled, the broad resonance collapsed into the baseline (~273 K), and by 193 K, the spectrum displayed a number of sharp singlets. The following major peaks are attributed to the isopropyl groups of $Ce_4O(O^iPr)_{13}(HO^iPr)$: δ −7.96, −6.56, −4.60, −1.36, 0.61, 4.60 (intensity ~1:1:1:1:2:1, C*H*); δ −4.29, −2.10, −0.42, 1.57, 5.91, 6.34, 7.96

* To whom correspondence should be addressed at Indiana University.

(1) Richardson, W. H. In *Oxidation in Organic Chemistry*; Wiberg, K. B., Ed.; Academic Press: New York, 1965; p 24.
(2) Ho, T. *Synthesis* **1973**, 347.
(3) Tomioka, H.; Oshima, K.; Nozaki, H. *Tetrahedron Lett.* **1982**, 539.
(4) Kanemoto, S.; Tomioka, H.; Oshima, K.; Nozaki, H. *Bull. Chem. Soc. Jpn.* **1986**, *59*, 105.
(5) Sheldon, R. A.; Kochi, J. K. *J. Am. Chem. Soc.* **1968**, 90, 6688.
(6) Adamson, A. W.; Fleischauer, P. D. p 252 In *Concepts of Inorganic Photochemistry*; Wiley: New York, 1975; p 252.
(7) Benrath, A.; Ruland, K. *Z. Anorg. Chem.* **1920**, *114*, 267.
(8) Bradley, D. C.; Chatterjee, A. K.; Wardlaw, W. *J. Chem. Soc.* **1956**, 2260; *Ibid.* **1957**, 2600.
(9) Vaartstra, B. A.; Huffman, J. C.; Gradeff, P. S.; Hubert-Pfalzgraf, L. G.; Daran, J.-C.; Parraud, S.; Yunlu, K.; Caulton, K. G. *Inorg. Chem.* **1990**, *29*, 3126.

0020-1669/91/1330-2317$02.50/0

Table I. Crystallographic Data for $Ce_4O(O^iPr)_{13}(^iPrOH)$

chem formula	$C_{42}H_{98}Ce_4O_{15}$	space group	$C2/c$
a, Å	21.405 (6)	T, °C	−130 °C
b, Å	14.077 (3)	λ, Å	0.71069
c, Å	20.622 (6)	ρ_{calcd}, g cm^{-3}	1.546
β, deg	103.97 (1)	μ(Mo Kα), cm^{-1}	30.6
V, Å^3	6029.75	R	0.0492
Z	4	R_w	0.0499
fw	1403.71		

Table II. Fractional Coordinates[a] and Isotropic Thermal Parameters[b] for $Ce_4O(O^iPr)_{13}(^iPrOH)$

	x	y	z	$10B_{iso}$, Å^2
Ce(1)	5610.9 (3)	2933.2 (4)	6795.5 (3)	21
Ce(2)	5728.2 (3)	1387.4 (4)	8212.2 (3)	21
O(3)	5000*	2551 (6)	7500*	18
O(4)	5468 (3)	1186 (4)	6959 (3)	19
C(5)	5745 (5)	437 (7)	6638 (5)	24
C(6)	5505 (5)	511 (7)	5889 (5)	34
C(7)	6483 (5)	478 (8)	6856 (6)	37
O(8)	6349 (3)	2504 (5)	7773 (3)	29
C(9)	6900 (6)	3014 (11)	8104 (12)	97
C(10)	6770 (8)	3936 (12)	8357 (7)	67
C(11)	7469 (6)	2702 (13)	7976 (7)	67
O(12)	4645 (3)	2507 (5)	6095 (3)	26
C(13)	4273 (5)	2868 (8)	5469 (5)	32
C(14)	4442 (6)	3897 (8)	5400 (5)	38
C(15)	4385 (7)	2259 (9)	4901 (5)	47
O(16)	6193 (3)	2785 (5)	6119 (3)	29
C(17)	6571 (5)	2742 (8)	5638 (6)	36
C(18)	6379 (6)	3551 (9)	5147 (6)	42
C(19)	7264 (6)	2758 (10)	5986 (6)	48
O(20)	5617 (3)	4405 (5)	6872 (3)	31
C(21)	5704 (8)	5379 (10)	6924 (6)	63
C(22)	5140 (9)	5937 (10)	6570 (8)	72
C(23)	6302 (9)	5670 (12)	6753 (10)	88
O(24)	5561 (3)	−255 (5)	8015 (3)	26
C(25)	5907 (5)	−1078 (8)	8325 (5)	34
C(26)	5585 (6)	−1498 (9)	8819 (6)	44
C(27)	6018 (6)	−1773 (9)	7816 (6)	46
O(28)	6505 (3)	997 (5)	9013 (3)	34
C(29)	7031 (7)	771 (13)	9536 (8)	77
C(30)	6905 (6)	−4 (10)	9967 (6)	48
C(31)	7595 (8)	1052 (18)	9546 (15)	160

[a] Fractional coordinates are × 10^4 for non-hydrogen atoms and × 10^3 for hydrogen atoms. An asterisk denotes a position fixed by symmetry. [b] Isotropic values for those atoms refined anisotropically are calculated by using the formula given by: Hamilton, W. C. *Acta Crystallogr.* **1959**, *12*, 609.

(intensity 6:6:6:6:6:6:6, CH_3). Minor peaks are less than 10% of these, and these may be due to the second species (A) detected by EPR spectroscopy.

Magnetic Studies. Magnetic susceptibility experiments were carried out on an SHE Model 905 SQUID magnetometer. The samples were powdered, weighed, and sealed into previously calibrated containers in an inert-atmosphere glovebox. Applied fields of 0.5 and 2.0 T and temperatures between 5 and 300 K were used for the measurements. EPR measurements at X-band were made at approximately 4 K with a Varian Model E-101 microwave bridge and an electromagnet with 12-in. pole faces. Liquid-helium temperatures were obtained by use of an Oxford Instruments ESR10 continuous-flow cryostat.

The EPR spectra both of $Ce_4O(O^iPr)_{13}(^iPrOH)$ (Figure 1) and of $Ce_2(O^iPr)_8(^iPrOH)_2$ were measured as powders at 4 K. While a very weak spectrum was seen due to impurities in apparently pure samples of the latter compound (Ce(IV), f^0), this spectrum makes no significant contribution to lines B and C in Figure 1.

X-ray Diffraction Study of $Ce_4O(O^iPr)_{13}(^iPrOH)$. A crystal of suitable size was cleaved from a large piece of the sample in a N_2-atmosphere glovebag. The crystal was mounted by using silicone grease and was then transferred to a goniostat where it was cooled to −130 °C for characterization and data collection.[10] A systematic search of a limited hemisphere of reciprocal space revealed intensities with Laue symmetry and systematic absences consistent with space group $C2/c$, which was later confirmed by the successful solution of the structure. Following intensity data collection ($6° < 2\theta < 45°$; see Table I), data processing gave a residual of 0.051 for the averaging of 794 unique intensities that had been observed more than once. Four standards measured for every 300 data showed no significant trends. No correction was made for absorption.

The structure was solved by a combination of direct methods (MULTAN78) and Fourier techniques. The metal positions were obtained from an initial E map, and the remainder of the non-hydrogen atoms was found in subsequent iterations of least-squares refinement and difference Fourier calculations. Hydrogen atoms were included in calculated positions to improve the refinement of the non-hydrogen atoms, but the hydrogens were not refined. Hydrogen thermal parameters were fixed at a value one larger than the isotropic thermal parameter of the atom to which they are bonded. The final difference Fourier had Ce residuals of 0.60–1.75 e/Å^3. All other residual peaks are less than 0.60 e/Å^3. There was no evidence for the hydroxyl hydrogen.

The results of the structure determination are shown in Table II and III and Figure 2. Further details are available as supplementary material.

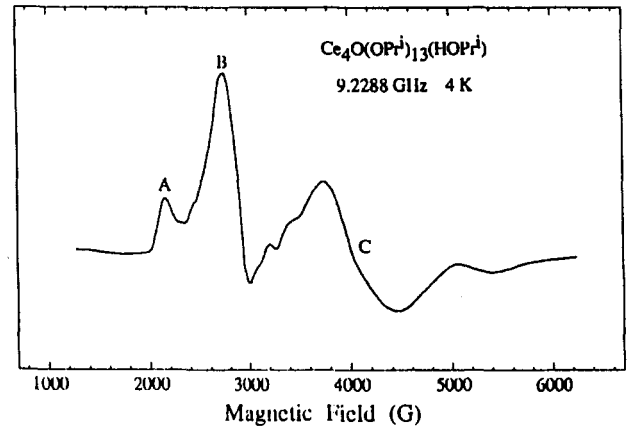

Figure 1. EPR spectrum of $Ce_4O(O^iPr)_{13}(^iPrOH)$ powder at 4 K.

Table III. Selected Bond Distances (Å) and Angles (deg) for $Ce_4O(O^iPr)_{13}(^iPrOH)$

Ce(1)–Ce(1)′	4.353 (1)	Ce(1)–O(16)	2.093 (7)
Ce(2)–Ce(2)′	3.732 (1)	Ce(1)–O(20)	2.078 (7)
Ce(1)–Ce(2)	3.603 (1)	Ce(2)–O(3)	2.483 (5)
Ce(1)–Ce(2)′	3.596 (1)	Ce(2)–O(4)′	2.514 (6)
O(24)–O(24)′	2.794 (10)	Ce(2)–O(4)	2.524 (6)
Ce(1)–O(3)	2.2419 (21)	Ce(2)–O(8)	2.374 (7)
Ce(1)–O(4)	2.511 (6)	Ce(2)–O(12)′	2.390 (6)
Ce(1)–O(8)	2.322 (6)	Ce(2)–O(24)	2.360 (7)
Ce(1)–O(12)	2.298 (6)	Ce(2)–O(28)	2.113 (7)

Ce(2)–Ce(1)–Ce(2)′	62.45 (3)	O(4)–Ce(2)–O(24)	74.14 (20)
Ce(1)–Ce(2)–Ce(1)′	74.42 (2)	O(4)′–Ce(2)–O(24)	76.00 (20)
Ce(1)–Ce(2)–Ce(2)′	58.68 (3)	O(4)–Ce(2)–O(28)	135.09 (24)
Ce(1)′–Ce(2)–Ce(2)′	58.86 (4)	O(4)′–Ce(2)–O(28)	131.52 (24)
O(3)–Ce(1)–O(4)	64.46 (24)	O(8)–Ce(2)–O(12)′	95.14 (23)
O(3)–Ce(1)–O(8)	75.88 (18)	O(8)–Ce(2)–O(24)	131.20 (22)
O(3)–Ce(1)–O(12)	76.54 (16)	O(8)–Ce(2)–O(28)	93.60 (25)
O(3)–Ce(1)–O(16)	160.4 (3)	O(12)′–Ce(2)–O(24)	133.67 (22)
O(3)–Ce(1)–O(20)	100.6 (3)	O(12)′–Ce(2)–O(28)	91.03 (25)
O(4)–Ce(1)–O(8)	73.01 (21)	O(24)–Ce(2)–O(28)	86.45 (24)
O(4)–Ce(1)–O(12)	73.05 (21)	Ce(1)–O(3)–Ce(1)′	152.3 (4)
O(4)–Ce(1)–O(16)	95.97 (23)	Ce(1)–O(3)–Ce(2)	99.23 (11)
O(4)–Ce(1)–O(20)	164.85 (24)	Ce(1)–O(3)–Ce(2)′	98.97 (11)
O(8)–Ce(1)–O(12)	142.98 (23)	Ce(2)–O(3)–Ce(2)′	97.4 (3)
O(8)–Ce(1)–O(16)	99.40 (25)	Ce(1)–O(4)–Ce(2)	91.37 (19)
O(8)–Ce(1)–O(20)	101.73 (25)	Ce(1)–O(4)–C(5)	125.1 (5)
O(12)–Ce(1)–O(16)	98.36 (25)	Ce(2)–O(4)–Ce(2)′	95.59 (19)
O(12)–Ce(1)–O(20)	107.23 (25)	Ce(2)–O(4)–C(5)	122.5 (5)
O(16)–Ce(1)–O(20)	98.94 (28)	Ce(2)′–O(4)–C(5)	122.3 (5)
O(3)–Ce(2)–O(4)	61.09 (16)	Ce(1)–O(8)–Ce(2)	100.20 (23)
O(3)–Ce(2)–O(4)′	61.23 (16)	Ce(1)–O(8)–C(9)	127.1 (10)
O(3)–Ce(2)–O(8)	70.55 (18)	Ce(2)–O(8)–C(9)	129.3 (11)
O(3)–Ce(2)–O(12)′	70.47 (18)	Ce(1)–O(12)–Ce(2)′	100.17 (22)
O(3)–Ce(2)–O(24)	119.79 (21)	Ce(1)–O(12)–C(13)	133.8 (6)
O(3)–Ce(2)–O(28)	153.74 (25)	Ce(2)′–O(12)–C(13)	125.4 (6)
O(4)–Ce(2)–O(4)′	82.96 (20)	Ce(1)–O(16)–C(17)	176.2 (7)
O(4)–Ce(2)–O(8)	71.93 (21)	Ce(1)–O(20)–C(21)	172.7 (9)
O(4)′–Ce(2)–O(8)	131.73 (20)	Ce(2)–O(24)–C(25)	132.2 (6)
O(4)–Ce(2)–O(12)′	131.49 (20)	Ce(2)–O(28)–C(29)	177.7 (8)
O(4)′–Ce(2)–O(12)′	71.51 (20)		

(10) Huffman, J. C.; Lewis, L. N.; Caulton, K. G. *Inorg. Chem.* **1980**, *19*, 2755.

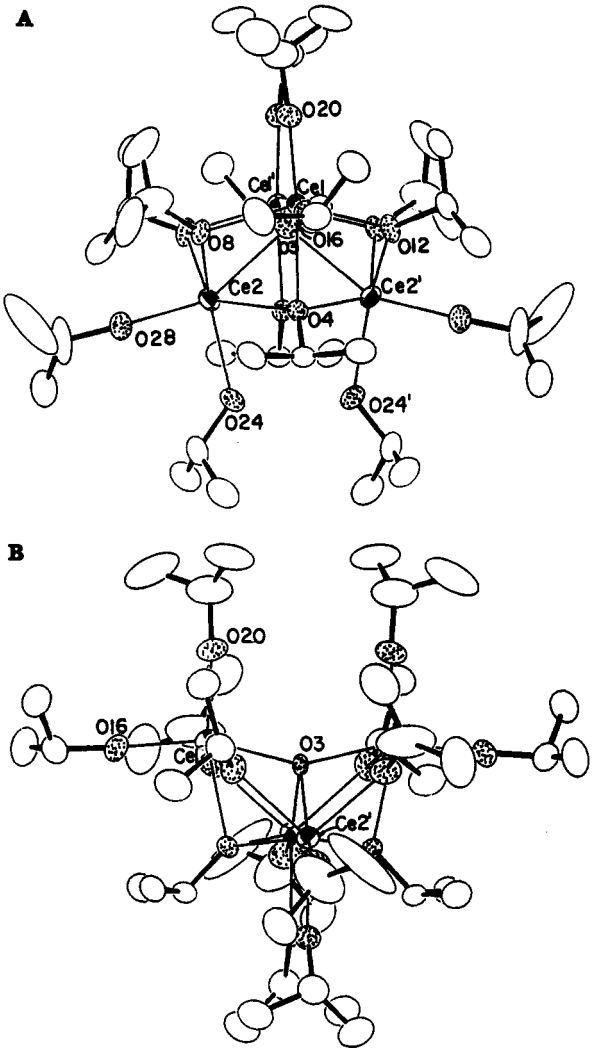

Figure 2. ORTEP drawings of the non-hydrogen atoms of $Ce_4O(O^iPr)_{13}(^iPrOH)$ with selected atom labeling, where (A) shows the bending at O(24) and O(24)′ to form a hydrogen bond between them and (B) shows the linearity at O(16) and O(20). The crystallographic C_2 axis (which creates primed from unprimed atoms) lies vertically in both drawings. Oxygens are stippled.

Results

Synthesis. The compound $Ce_2(O^iPr)_8(^iPrOH)_2$ (I) is remarkably photosensitive, both in solution and in the solid state. The

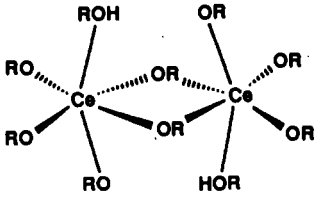

I

bright yellow compound I, which exhibits intramolecular hydrogen bonding between alcohol and alkoxide ligands, turns orange-brown even in room light. From the resulting solution in DME/isopropyl alcohol can be isolated a paramagnetic solid, II. This observation alone shows that photolysis effects a redox process, since I is diamagnetic (f^0).

Irradiation (sunlight) of yellow solid $Ce_2(O^iPr)_8(^iPrOH)_2$ for 15 h similarly yields a orange-brown, almost black, solid whose metal weight percent is identical with that of the product from solution photolysis. The solid-state photolysis also results in accumulation of a colorless liquid identified as isopropyl alcohol (^1H NMR).

Table IV. Magnetic Susceptibility Data for $Ce_4O(O^iPr)_{13}(^iPrOH)$

H, kG	T, K	C	θ, K	μ_{eff}, μ_B
5, 20	80–300	0.9110 ± 0.0092	−72.23 ± 2.67	2.699 ● 0.014
5, 20	5–40	0.4182 ● 0.0113	−2.38 ± 0.74	1.829 ● 0.025

The elemental analysis of the product is consistent with the formula $Ce_4O(O^iPr)_{13}(^iPrOH)$. It is soluble in toluene, *n*-pentane, $MeOC_2H_4OMe$, THF, ^iPrOH, and $CHCl_3$. The compound has no clear melting point, but appears to decompose near 180 °C. Attempted sublimation (up to 300 °C at 10^{-3} Torr) is unsuccessful. The compound is very air-sensitive; the dark color changes to yellow within 10 s of exposure of the solid to air. The infrared spectrum of $Ce_4O(O^iPr)_{13}(^iPrOH)$ in Nujol shows a weak ν(O–H) band at 3150 cm^{-1}. This low value is indicative of hydrogen bonding.

Solid-State Structure. Compound II was identified by X-ray diffraction as $Ce_4O(O^iPr)_{13}(^iPrOH)$. The molecule is of the butterfly form (Figure 2) and possesses a crystallographic C_2 axis. The wingtips of the butterfly are connected to an oxide oxygen (O(3)), which is μ_4-coordinated by virtue of bonding also to both hinge cerium centers. Compared to most $M_4(\mu_4\text{-}X)$ butterfly structures,[11] $Ce_4O(O^iPr)_{13}(^iPrOH)$ is unusual in having the μ_4-X group very "concave" (drawn toward the hinge).

This structure yields coordination number 6 for the wingtip metals, Ce(1), but coordination number 7 for the two hinge atoms, Ce(2). This is satisfied via four μ_2- and two μ_3-O^iPr groups, as well as by eight terminal ligands. The assignment of $^iPrO^-$ and ^iPrOH groups among the terminal ligands from the solid-state structure is possible, even given that we were not able to conclusively locate the hydroxylic proton. All terminal Ce–O distances are shorter than 2.11 Å except Ce–O(24), which is 2.360 (7) Å. All terminal Ce–O–C angles are 172° except Ce(2)–O(24)–C(25), which is 132.2°. These conclusively localize the proton on the O(24)/O(24)′ pair, which are related by a crystallographic C_2 axis. Moreover, these two oxygens lean toward one another: the angle Ce(2)′–Ce(2)–O(24) is 78.5 (1)°, and the O(24)′/O(24) distance (2.79 Å) is much shorter than the Ce(2)/Ce(2)′ distance (3.732 Å). These features are characteristic[9] of intramolecular hydrogen bonding between *one* alkoxide and *one* alcohol ligand. We conclude that there is only one[12] proton between O(24) and O(24)′. Since the thermal parameters of O(24) are not particularly elongated, there is no evidence for disorder between totally distinct alcohol and alkoxide O^iPr groups. We conclude that the single proton must lie *very near* the crystallographic C_2 axis. *The hydrogen bond is nearly symmetric.*

A consequence of establishing the molecular formula to be $Ce_4O(O^iPr)_{13}(^iPrOH)$ is that this explains the observed paramagnetism (and the intense color): the molecule is a mixed-valence species. The symmetry in the solid state rules out a localized $Ce^{III}Ce^{IV}_3$ formulation. The compound must have a delocalized $Ce^{IV}_2(Ce_2^{7+})$ assignment, or else Ce_4^{15+}. The high air sensitivity of the compound is, however, explained by the presence of some cerium below oxidation state +4.

Magnetic Studies. The magnetic susceptibility was measured between 5 and 300 K. No field dependence of χ was observed at 0.5 and 2.0 T. Two linear regions in the $1/\chi$ vs T plot have been fit to the Curie–Weiss equation $\chi = C(T-\theta)^{-1}$. Parameters derived from this fit are given in Table IV. The observed paramagnetism provides independent support for the conclusion, derived from X-ray diffraction, that the compound contains Ce(III). The values of μ_{eff} in the two temperature domains, 1.83 μ_B (5–40 K) and 2.70 μ_B (80–300 K), are comparable to the values for a variety of mononuclear Ce(III) compounds at 300 K (1.8–2.5 μ_B)[13,14] and also with a variable-temperature study of

(11) Bradley, J. S. *Adv. Organomet. Chem.* **1983**, *22*, 1. Gladfelter, W. *Adv. Organomet. Chem.* **1985**, *24*, 41. Schauer, C. K.; Shriver, D. F. *Angew. Chem., Int. Ed. Engl.* **1987**, *26*, 255. Housecroft, C. E.; Buhl, M. L.; Long, G. J.; Fehlner, T. P. *J. Am. Chem. Soc.* **1987**, *109*, 3323. Rath, N. P.; Fehlner, T. P. *J. Am. Chem. Soc.* **1987**, *109*, 5273. Bottomley, F.; Sutin, L. *Adv. Organomet. Chem.* **1988**, *28*, 339.

(12) If there were two hydrogens, the H/H distance in such a $Ce_2(HOR)_2$ group would be less than 1.5 Å. This is too short to be realistic.

(^{t}BuC$_5$H$_4$)$_3$Ce (2.28 μ_B from 50 to 280 K).[15]

To obtain independent evidence for the presence of one (or more) paramagnetic species in the solid state, the EPR spectrum of $Ce_4O(O^iPr)_{13}(^i$PrOH) powder was measured at 4 K. The spectrum is complex and broad. If the features labeled B and C in Figure 1 are assigned to a single species, B can be assigned to $g_\parallel$ and C to $g_\perp$. The resulting g values (2.41 and 1.64, respectively) yield a g_{av} of 1.90, which predicts μ_{eff} = 1.65 for this $S = {}^1/_2$ species. These g values obtained for the major EPR-active species can account for most of the paramagnetism measured by the susceptibility experiment, and thus we assign both properties to $Ce_4O(O^iPr)_{13}(^i$PrOH). This μ_{eff} is about 10% lower than that (1.83 μ_B) obtained from low-temperature susceptibility measurement. The feature labeled A in the EPR spectrum may belong to a second, minor species whose other features may be masked by the strong EPR signal of the major species. Nevertheless it will contribute to the bulk magnetic susceptibility measurement and may account for some of the discrepancies between the EPR and susceptibility values of the effective magnetic moments at low temperature.

Structure in Solution. We have investigated the variable-temperature ^{1}H NMR spectra of $Ce_4O(O^iPr)_{13}(^i$PrOH) in toluene as a source of information about solution behavior and integrity of this molecule. At 305 K (500 MHz) one sees only a very broad resonance centered at 0.2 ppm, together with a sharp intensity peak at 6.0 ppm. The latter we assign to the hydroxyl proton. At 298 K, the broad peak is even broader. At 193 K, the dynamic processes responsible for the above simple spectra have slowed. The resonances span a relatively narrow chemical shift range (+16 to −8 ppm). One sees six peaks assigned to methine hydrogens of intensity 1:1:1:1:1:2. This is in agreement with the solid-state structure A, under the assumption of C_{2v} symmetry or its time-

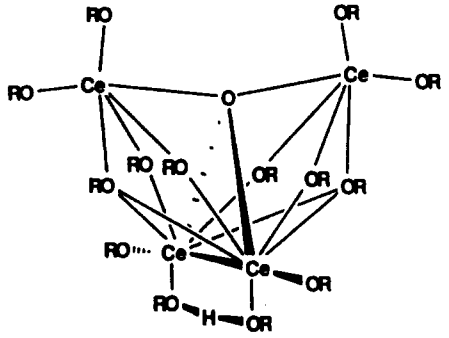

A

averaged equivalent; this implies a symmetric hydrogen bond or rapid migration of the hydroxyl proton between the two hinge OR groups. One also sees a number of peaks whose intensity is consistent with their being due to methyl protons. Structure A requires seven such environments; one observes six such peaks, and a seventh peak lies among the methyl resonances of $Ce_2(O^iPr)_8(^i$PrOH)$_2$, present as an impurity. While the methyl and methine resonances are too broad to show H/H coupling, they are quite sharp (full width at half-height 10–15 Hz for methyl and 20–50 Hz for methine) for a paramagnetic species. The hydroxyl proton resonance remains relatively sharp as the temperature is lowered. The final conclusion from these observations is that $Ce_4O(O^iPr)_{13}(^i$PrOH) retains its solid-state structure in toluene solution but that proton transfer and site exchange among alkoxide groups occurs at a rate of $\sim 10^4$ s^{-1} at 30 °C.

The NMR signals (both ^{1}H and ^{13}C) of $Ce_4O(O^iPr)_{13}(^i$PrOH) are relatively sharp and only modestly displaced from what would be seen for O^{i}Pr groups in a diamagnetic environment. This is particularly impressive for the methine carbons and hydrogens, which are only two and three bonds removed, respectively, from cerium. This is consistent with dipolar interaction as the source of these chemical shifts.

Thermal Reactivity of $Ce_2(O^iPr)_8(^i$PrOH)$_2$. The conversion of $Ce_2(O^iPr)_8(^i$PrOH)$_2$ to $Ce_4O(O^iPr)_{13}(^i$PrOH) requires photolysis. Attempts to effect this conversion thermally (110 °C, 15 days) in DME/^{i}PrOH in a tube wrapped in aluminum foil in an oven gave only a pale blue-gray precipitate in a gray solution. There was never an orange color during the thermolysis.

Influence of the Alkoxy R Group. Both the *n*-octyl and *sec*-butyl alkoxides of Ce(IV) are light sensitive. The conversion to the orange-brown color occurs faster than it does for the isopropoxide. DME solutions of cerium(IV) *tert*-butoxide, in contrast, undergo no color change after 36 h in sunlight. A toluene solution of $Ce(OSiPh_3)_4$(DME) is likewise unchanged in color after photolysis. Finally, photolysis of alcohol-free $[Ce(O^iPr)_4]_n$ in pure DME also gives the orange-brown product; the hydroxyl proton is not necessary for the conversion to a mixed-valence compound.

Mechanistic Conclusions. Taken together, these results show the necessity of an α-hydrogen for the reduction. That is, it must be possible to oxidize the alkoxide (to a ketone) if cerium is to be reduced. The absence of thermal redox conversion, and its occurrence upon photolysis, is consistent with light-activated Ce–O homolysis.

Discussion

Molecular Structure. Bond lengths from cerium to terminal isopropoxides (average 2.095 Å) are comparable to the corresponding values in $Cp^*_2Ce_2(O^tBu)_2(\mu$-O^{t}Bu)$_2$ (2.120 Å)[16] and $Ce_2(OCH^tBu_2)_6$ (2.147 Å).[17] To bridging alkoxides, the average values (2.346, 2.406 and 2.363 Å, respectively) are also similar. Among Ce(IV) compounds, there is a wider variation in Ce–O (terminal) distances (Å): 2.045 in Cp_3CeO^tBu,[18] 2.115 in Ce(OSiPh$_3$)$_4$(DME),[19] 2.025 in $Ce(O^tBu)_2(NO_3)_2(^t$BuOH)$_2$,[20] and 2.141 in $Na_2(DME)_2Ce(O^tBu)_5$.[20] The corresponding distance (2.222 Å) in $Ce(OSiPh_3)_3(THF)_3$[21] is long by any standard.

There is a distinct lengthening of Ce–O distances in $Ce_4O(O^iPr)_{13}(^i$PrOH) from terminal (2.095 Å) to μ_2-OR (2.346 Å) to μ_3-OR (2.516 Å). This has been noted before.[20] It is anticipated that this could influence C/O bond scission reactions.

The distance from Ce to the oxygens of the ^{i}PrOHO^{i}Pr$^-$ ligand, 2.360 Å, is very close to the average of the Ce–OR (terminal) distance and the Ce–[O(H)R] distance (2.53 Å) in $Ce(O^tBu)_2(NO_3)_2(^t$BuOH)$_2$.[20]

The Ce_4O core reported here is of the generic M_4X "butterfly" form, which has been extensively reported for X = B, C, and N.[11] The case for X = O^{2-} remained unknown until 1987, when $MnFe_3(\mu_4$-O)(CO)$_{12}^-$ was reported.[11] Also, recently reported were $Cp^*_4Ta_4(\mu_2$-O)$_4(\mu_3$-O)$_2(\mu_4$-O)(OH)$_2$[22] and $Y_4(\mu_4$-O)(O^{t}Bu)$_{10}Cl_2^{2-}$.[23] In none of these other oxo butterflies is the oxide drawn inward toward the hinge metals (here Ce(2)) so that the wingtip–O–wingtip angle is concave, as it is in $Ce_4O(O^iPr)_{13}(^i$PrOH). As a consequence of the concave character of the oxide location in the butterfly, the O–Ce (hinge) distance (2.242 Å) is considerably shorter than than O–Ce (wingtip) distance (2.483 Å).

For metals that strive for an octahedral coordination geometry, the M_3X_{11} structural motif B is of frequent occurrence: $M_3O(O^tBu)_{10}$ (M = Ce,[20] U[24]). This structure uses μ_3-ligands to satisfy

(13) Fischer, R. D. In *Fundamental and Technological Aspects of Organo-f-Element Chemistry*; Marks, T. J., Fragola, I., Eds.; D. Reidel: Dordrecht, The Netherlands, 1985; p 277.
(14) Evans, W. J.; Hozbor, M. A. *J. Organomet. Chem.* **1987**, *326*, 299.
(15) Stults, S. D.; Andersen, R. A.; Zalkin, A. *Organometallics* **1990**, *9*, 115.
(16) Heeres, H. J.; Teuben, J. H.; Rogers, R. D. *J. Organomet. Chem.* **1989**, *364*, 87.
(17) Stecher, H. A.; Sen, A.; Rheingold, A. *Inorg. Chem.* **1987**, *27*, 1130; *Ibid.* **1989**, *28*, 3280.
(18) Evans, W. J.; Deming, T. J.; Ziller, J. W. *Organometallics* **1989**, *8*, 1581.
(19) Gradeff, P. S.; Yunlu, K.; Gleizes, A.; Galy, J. *Polyhedron* **1989**, *8*, 1001.
(20) Evans, W. J.; Deming, T. J.; Olofson, J. M.; Ziller, J. W. *Inorg. Chem.* **1989**, *28*, 4027.
(21) Gradeff, P. S.; Yunlu, K.; Deming, T. J.; Olofson, J. M.; Doedens, R. J.; Evans, W. J. *Inorg. Chem.* **1990**, *29*, 420.
(22) Gibson, V. C.; Kee, T. P. *J. Chem. Soc., Chem. Commun.* **1990**, 29.
(23) Evans, W. J.; Sollberger, M. S.; Hanusa, T. P. *J. Am. Chem. Soc.* **1988**, *110*, 1841.

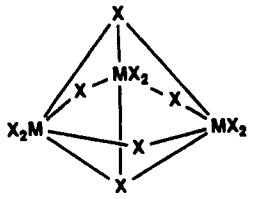

B

the coordination sphere of three metals. The Ce_4O core reported here is clearly related to the M_3X_{11} motif by the grafting of a fourth MX_3 unit onto the M_3X_{11} core to form a wingtip of the butterfly (see C, where dashed lines indicate newly formed bonds).

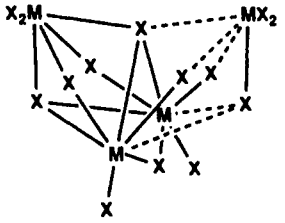

C

The coordination sphere shown in C is finally expanded to include one molecule of parent alcohol. The Lewis acidity of $Ce_4O(OR)_{13}$ is thus established, and the frequent occurrence of coordinated alcohol[9] is further extended. Since $Ce_4O(O^iPr)_{13}(^iPrOH)$ contains one Ce^{III} and three Ce^{IV} ions, this formal analysis of the parentage of the Ce_4O core in terms of $Ce^{IV}{}_3O$ (cf. $Ce_3O(O^tBu)_{10}$) and Ce^{III} constituents may have some relevance to its mechanism of formation.

Origin of the Reduction. Sheldon and Kochi[5] established that the photochemical reduction of Ce(IV) (as their carboxylates) involved the intermediacy of alkyl radicals (from decarboxylation of carboxyl radicals). Photochemical homolysis of the $Ce-O_2CR$ bond was suggested. The necessity of primary or secondary alkoxy groups in the synthesis of $Ce_4O(OR)_{13}(ROH)$ suggests that hydrogen transfer from a geminate alkoxy radical also participates here. The resulting cerium(IV) hydride presumably then forms H_2 and Ce(III).

Seeking the Source of the Oxo Ligand. To establish whether isopropoxide is the source of the μ_4-O atom, we have examined the volatile reaction products. After irradiation of $Ce_2(O^iPr)_8(^iPrOH)_2$ in C_6D_6, the volatiles were quantitatively vacuum-transferred (-196 °C) to an NMR tube and analyzed by ^1H NMR spectroscopy. This showed ^{i}PrOH and acetone (the source of the reducing equivalents) but neither resonance of propane and no signals in the vinyl region (e.g., propylene). In another instance of oxo formation we have detected significant amounts of propane by this procedure.[25]

Acknowledgment. This work was supported by DOE Grant DE-FG02-88ER13906. We thank Scott Horn for skilled technical assistance.

Supplementary Material Available: Listings of full crystallographic details and anisotropic thermal parameters (2 pages); a table of observed and calculated structure factors (9 pages). Ordering information is given on any current masthead page.

(24) Cotton, F. A.; Marler, D. O.; Schwotzer, W. *Inorg. Chim. Acta* **1984**, *95*, 207.

(25) Vaartstra, B. A.; Streib, W. E.; Caulton, K. G. *J. Am. Chem. Soc.* **1990**, *112*, 8593.

Contribution from the Department of Chemistry
Texas A&M University, College Station, Texas 77843-3255

Utility of Semilocalized Bonding Schemes in Extended Systems: Three-Center Metal-Metal Bonding in MoS_2, $H_x(Nb,Ta)S_2$, and ZrS

Kyeong Ae Yee and Timothy Hughbanks*

Received October 9, 1990

A semilocalized description of bonding in extended metal-metal-bonded systems is described for the prototype title compounds. Beginning with calculated band orbitals, we explicitly construct three-center bond orbitals (Wannier functions) for the trigonal-prismatic layer compound MoS_2. While no well-localized single-center functions or two-center bonds can be constructed, the three-center Wannier functions prove to be highly localized. The isoelectronic $LiNbO_2$ can be treated similarly. This provides a very economical description of the M-M bonding in these layer compounds and is shown to be the most natural way of understanding the metal-hydrogen and residual metal-metal bonding in the tantalum and niobium hydrogen bronzes $H_x(Ta,Nb)S_2$. ZrS adopts a WC structure that may be viewed as a 3-D condensation of the 2-D trigonal-prismatic layers present in the aforementioned materials. The 2-D metal-metal bonding description in the layers persists in ZrS as well, in agreement with earlier work by Nguyen and co-workers.

Introduction

In the description of the electronic structure of solids and surfaces there is a widely recognized tension between localized and delocalized bonding viewpoints. In the vernacular of the field it comes down to a dilemma that pits the traditional physicists' delocalized *bands* against the chemists' *bonds*. This situation is familiar to chemists in the contrast between valence bond and molecular orbital theories. While these two approaches differ in several respects, perhaps the most important conceptual difference between the theories lies in the localized nature of the valence bond approach and the delocalization of molecular orbitals. In the intermediate regime are semilocalized descriptions of bonding wherein the multicenter bonding schemes provide chemists a means of "counting electrons" and assigning electron pairs to some combination of two-center-two-electron (Lewis) bonds and, e.g., three-center-two-electron (3c-2e)[1] or three-center-four-electron (3c-4e) systems.[2,3]

The need for chemically useful yet physically realistic localized bonding schemes for solids continues to press. In the present paper, we present some results of our efforts to understand the electronic structures of manifestly extended systems, especially those involving metal-metal bonds. We extract localized orbitals from delocalized band orbitals, using well-known Wannier functions[4-7]

* To whom correspondence is to be addressed.

(1) Lipscomb, W. N. *Boron Hydrides*; Benjamin: New York, 1963.
(2) Pimentel, G. C. *J. Chem. Phys.* **1951**, *19*, 446.
(3) Rundle, R. E. *J. Am. Chem. Soc.* **1963**, *85*, 112.
(4) Wannier, G. H. *Phys. Rev.* **1937**, *52*, 191.

0020-1669/91/1330-2321$02.50/0